Limited proteolysis as a structural probe of the soluble alpha-glycerophosphate oxidase from Streptococcus sp.

ARTICLE *in* BIOCHEMISTRY · JUNE 2000

Impact Factor: 3.02 · Source: PubMed

4 AUTHORS, INCLUDING:

Derek Parsonage
Wake Forest School of Medicine
92 PUBLICATIONS **2,421** CITATIONS
SEE PROFILE

Al Claiborne
Wake Forest School of Medicine
73 PUBLICATIONS **1,143** CITATIONS
SEE PROFILE

Limited Proteolysis as a Structural Probe of the Soluble α-Glycerophosphate Oxidase from *Streptococcus* sp.†

Véronique Charrier,‡,§ James Luba,‡ Derek Parsonage, and Al Claiborne*

Department of Biochemistry, Wake Forest University Medical Center, Winston−Salem, North Carolina 27157

Received October 28, 1999; Revised Manuscript Received February 11, 2000

ABSTRACT: As reported previously [Parsonage, D., Luba, J., Mallett, T. C., and Claiborne, A. (1998) *J. Biol. Chem. 273*, 23812−23822], the flavoprotein α-glycerophosphate oxidases (GlpOs) from a number of enterococcal and streptococcal sources contain a conserved 50−52 residue insert that is completely absent in the homologous α-glycerophosphate dehydrogenases. On limited proteolysis with trypsin, the GlpO from *Streptococcus* sp. ($m = 67.6$ kDa) is readily converted to two major fragments corresponding to masses of approximately 40 and 23 kDa. The combined application of sequence and mass spectrometric analyses demonstrates that the 40-kDa fragment represents the N-terminus of intact GlpO (Met1−Lys368; 40.5 kDa), while the 23-kDa band represents a C-terminal fragment (Ala405−Lys607; 22.9 kDa). Hence, limited proteolysis in effect excises most of the GlpO insert (Ser355−Lys404), indicating that this represents a flexible region on the protein surface. The active-site and other spectroscopic properties of the enzyme, including both flavin and tryptophan fluorescence spectra, titration behavior with both dithionite and sulfite, and preferential binding of the anionic form of the oxidized flavin, were largely unaffected by proteolysis. Enzyme-monitored turnover analyses of the intact and nicked streptococcal GlpOs (at [GlpO] ∼10 μM) demonstrate that the single major catalytic defect in the nicked enzyme corresponds to a 20-fold increase in K_m(Glp); the basis for this altered kinetic behavior is derived from an 8-fold decrease in the second-order rate constant for reduction of the nicked enzyme, as measured in anaerobic stopped-flow experiments. These results indicate that the flexible surface region represented by elements of the GlpO insert plays an important role in mediating efficient flavin reduction.

In contrast to the membrane-associated flavoprotein GlpD[1] which catalyzes the oxidation of Glp → DHAP with concomitant reduction of ubiquinone (*1*), the soluble GlpO catalyzes the direct reduction of $O_2 \rightarrow H_2O_2$ (*2*). This functional distinction is critical in lactic acid bacteria such as the enterococci and streptococci, since these heme-deficient organisms lack the membrane-associated respiratory chains found in other bacteria and in mitochondria (*3*). Despite this functional distinction, the GlpO sequences from *Enterococcus casseliflavus* and two other streptococcal sources compare favorably (>30% identity) with those of several membrane-associated GlpDs from other bacterial and mitochondrial sources (*2*). While conserved regions are generally distributed over the entire sequence, the three GlpOs also contain a 52-residue insert (Ser356−Val407 in the *E. casseliflavus* enzyme), which has no counterpart in the GlpDs, and previous speculation focused on a possible role for this insert in contributing to the cytosolic localization of the soluble GlpO.

Apart from the N-terminal FAD-binding region shared by GlpO and GlpDs, the only other functional element identified in these sequences has been proposed to correspond to elements of the Glp-binding site in the aerobic GlpD from *Escherichia coli* (*1*). Similarities were noted within the region spanning residues 300−390 of this membrane-associated flavoprotein and elements of the DHAP-binding site of yeast TIM (*4*), which consists of a flexible loop and two shorter glycine-containing loops that together interact with and provide a lid for the phosphate end of the bound DHAP. To the extent that the comparable segments in the *Esc. coli* GlpD may thus serve in Glp binding, there are also some similarities between GlpD and GlpO within the regions of comparison. However, the alignment of the *E. casseliflavus* GlpO and *Esc. coli* GlpD sequences also places the 52-residue insert *between* the "flexible loop" and the two "glycine-containing loops" as defined in the TIM-DHAP structure (*2*). In the absence of a three-dimensional structure for either GlpO or any known GlpO homolog, there is really no detailed information concerning the true functional role of this insert and/or the determinants for Glp binding.

The previous study with the recombinant *E. casseliflavus* GlpO showed that the enzyme follows a ping-pong kinetic

† This work was supported by National Institutes of Health Grant GM-35394.

* To whom correspondence should be addressed. Telephone: (336) 716−3914. Fax: (336) 716-7671. URL: http://invader.bgsm.wfu.edu/.

‡ These authors contributed equally to this work.

§ Present address: Service de Biochimie, Hoechst Marion Roussel, 93235 Romainville Cedex, France.

[1] Abbreviations: Glp, α-glycerophosphate; GlpD, α-glycerophosphate dehydrogenase; GlpO, α-glycerophosphate oxidase; GlpO-*S*, *Streptococcus* sp. GlpO; DHAP, dihydroxyacetone phosphate; TIM, triosephosphate isomerase; CAPS, 3-cyclohexylamino-1-propanesulfonic acid; EGTA, [ethylenebis(oxyethylenenitrilo)]tetraacetic acid; TPCK, *N*-tosyl-L-phenylalanine chloromethyl ketone; SDS−PAGE, sodium dodecyl sulfate−polyacrylamide gel electrophoresis; ESI-MS, electrospray interface-mass spectrometry; HPLC, high-performance liquid chromatography; TFA, trifluoroacetic acid; DHOD, dihydroorotate dehydrogenase; DAAO, D-amino acid oxidase.

10.1021/bi992499j CCC: $19.00
Published on Web 04/05/2000

mechanism (*2*); analysis of the reductive half-reaction revealed a biphasic process in which k_{slow} was both $\ll k_{cat}$ and independent of the Glp concentration. These data were interpreted in terms of a two-state model for the resting oxidized enzyme in which the E-FAD* form is not able to bind Glp productively for reduction; conversion of E-FAD* → E-FAD at 4−5 s^{-1} (pH 7.0, 5 °C) is therefore limiting for this fraction of enzyme reduction. The reaction of Glp with E-FAD was consistent with the initial rapid equilibrium formation of an E-FAD·Glp complex (K_d = 25 mM), followed by reduction to yield E-$FADH_2$ + DHAP at k_{red} = 48 s^{-1} ($\sim k_{cat}$). While the structural features distinguishing the E-FAD* and E-FAD forms of GlpO remain unknown, a chance observation indicated that limited proteolysis could provide a useful structural probe for the resting oxidized enzyme. In this paper, we present the results of both equilibrium and kinetic analyses for the intact and nicked forms of GlpO from *Streptococcus* sp.

EXPERIMENTAL PROCEDURES

Materials and General Methods. CAPS and EGTA were purchased from Sigma, and ultrapure urea was from ICN. TPCK-trypsin was purchased from Worthington Biochemicals, and Immobilon-P transfer membranes were from Millipore. All other chemicals, as purchased from sources described previously (*2*, *5*), were of the best grades available. The recombinant GlpO from *E. casseliflavus* was purified as previously described (*2*), and the enzyme from *Streptococcus* sp. (GlpO-*S*) was purchased from Genzyme Diagnostics. The Genzyme preparation was purified to homogeneity in a single chromatographic step using Macro-Prep Ceramic Hydroxyapatite (Bio-Rad) under conditions similar to those described previously (*2*). A total of 200 mg of the lyophilized powder was dissolved in 10 mM potassium phosphate buffer, pH 7.0 (no EDTA), and dialyzed exhaustively against the same buffer. After the column was loaded and washed, the enzyme was eluted with a 10−250 mM phosphate gradient. The specific activity as measured in the standard spectrophotometric assay (*5*) with purified GlpO-*S* is 60.3 U/mg, A_{280}/A_{449} = 7.4, and ϵ_{449} = 11 200 M^{-1} cm^{-1}.

Limited Proteolysis. Analytical experiments were carried out by incubating 0.1 mg (1.5 nmol) of either GlpO or GlpO-*S* with trypsin (1:25 or 1:50 trypsin:GlpO, w/w; as required) in 50 μL of 50 mM Tris−SO_4^{2-}, pH 8.0, plus 1 mM $CaCl_2$, at either room temperature or 37 °C (see Results). Reactions were quenched by adding EGTA to a final concentration of 4 mM while chilling the sample on ice, and aliquots were analyzed by SDS−PAGE. Stopped-flow and spectral analyses of nicked GlpO-*S* required a preparative-scale proteolysis reaction with a combined volume of 11.9 mL while maintaining the concentration of GlpO-*S* at 2 mg/mL. These incubations were continued at room temperature for 30 min at a ratio of trypsin to GlpO-*S* of 1:25 (w/w) before quenching with EGTA. The nicked enzyme was then dialyzed into 50 mM potassium phosphate, pH 7.0, plus 0.5 mM EDTA with a CM-30 microconcentrator (Amicon); SDS−PAGE analyses before and after ultrafiltration demonstrated both the complete conversion of intact to nicked enzyme and the absence of any further change in the proteolysis profile during ultrafiltration. In this manner, approximately 25 mg of nicked GlpO-*S* could be prepared; the enzyme was stored overnight at 4 °C before stopped-flow and/or spectral work.

Protein Analysis Methods. SDS−PAGE analyses routinely employed 10% gels calibrated with the 10-kDa Protein Ladder standards (Gibco BRL). For N-terminal sequence analyses, GlpO proteolysis products that had been resolved by SDS−PAGE were transferred electrophoretically onto an Immobilon-P membrane, using the Mini Trans-Blot Cell (Bio-Rad) and following the protocol provided by PE Biosystems (*6*). After detection with Coomassie Blue R-250, bands of interest were excised and submitted for N-terminal sequence analysis by the Protein Analysis Core Laboratory, Comprehensive Cancer Center of Wake Forest University. To analyze for the presence of the GlpO-*S* proteolysis product corresponding to Ser369−Lys404 (calculated m = 4209 Da), SDS−PAGE was run with a 16.5% gel using the Tris−Tricine buffer system described by Bio-Rad (*7*) and the Peptide Marker Kit from Amersham Pharmacia Biotech. Both intact and nicked GlpO samples were prepared for ESI-MS analyses by dialyzing into deionized water with a CM-30 microconcentrator; these analyses were performed by the Analytical Chemistry Core Laboratory, Comprehensive Cancer Center of Wake Forest University. Calculated mass values for both intact GlpO and tryptic fragments were determined using the program MS-DIGEST available from the UCSF Mass Spectrometry Facility (*8*).

Spectral Analyses and Stopped-Flow Kinetics. Absorbance spectra were measured with Hewlett-Packard model 8452A and Beckman DU 7500 diode-array spectrophotometers, and fluorescence measurements were made with an SLM AB2 spectrofluorimeter, as previously described (*9*). Tryptophan fluorescence was determined at λ_{EX} = 295 nm (*10*) with a GlpO concentration of 1.2 μM. Titrations with dithionite and sulfite and other static spectral measurements followed established protocols (*2*). All rapid-reaction analyses were carried out with the Applied Photophysics DX.17 MV stopped-flow spectrophotometer (*11*), which has recently been upgraded to include an Acorn 32-bit RISC-processor workstation. Protocols for both enzyme-monitored turnover and reductive half-reaction experiments with GlpO, as well as data analysis methods, have been described in detail (*2*). Pro-Kineticist (Pro-K) data analysis routines (*11*) are run on a Silicon Graphics 320 workstation.

RESULTS

Streptococcus sp. GlpO. The source of GlpO-*S* is *Streptococcus* sp., and the DNA sequence for the gene was very kindly provided by Dr. Hideo Misaki and the Diagnostics Research and Development Department, Diagnostics Division, Asahi Chemical Industry Co., Ltd., Ohito, Japan. The enzyme as purchased from Genzyme Diagnostics was purified in a single chromatographic step as described in Experimental Procedures, and the m value for intact GlpO-*S* was determined by ESI-MS to be 67 594 ± 8 Da. This value is 21 Da higher than the calculated mass (67 573 Da) but could easily represent formation of a Na^+ adduct, which would add 23 Da to the measured m value. N-terminal analysis demonstrated that the protein sequence was identical to that deduced from the DNA sequence over the first 16 amino acid residues. Figure 1 presents a multiple sequence alignment for the *E. casseliflavus* and *Streptococcus* sp.

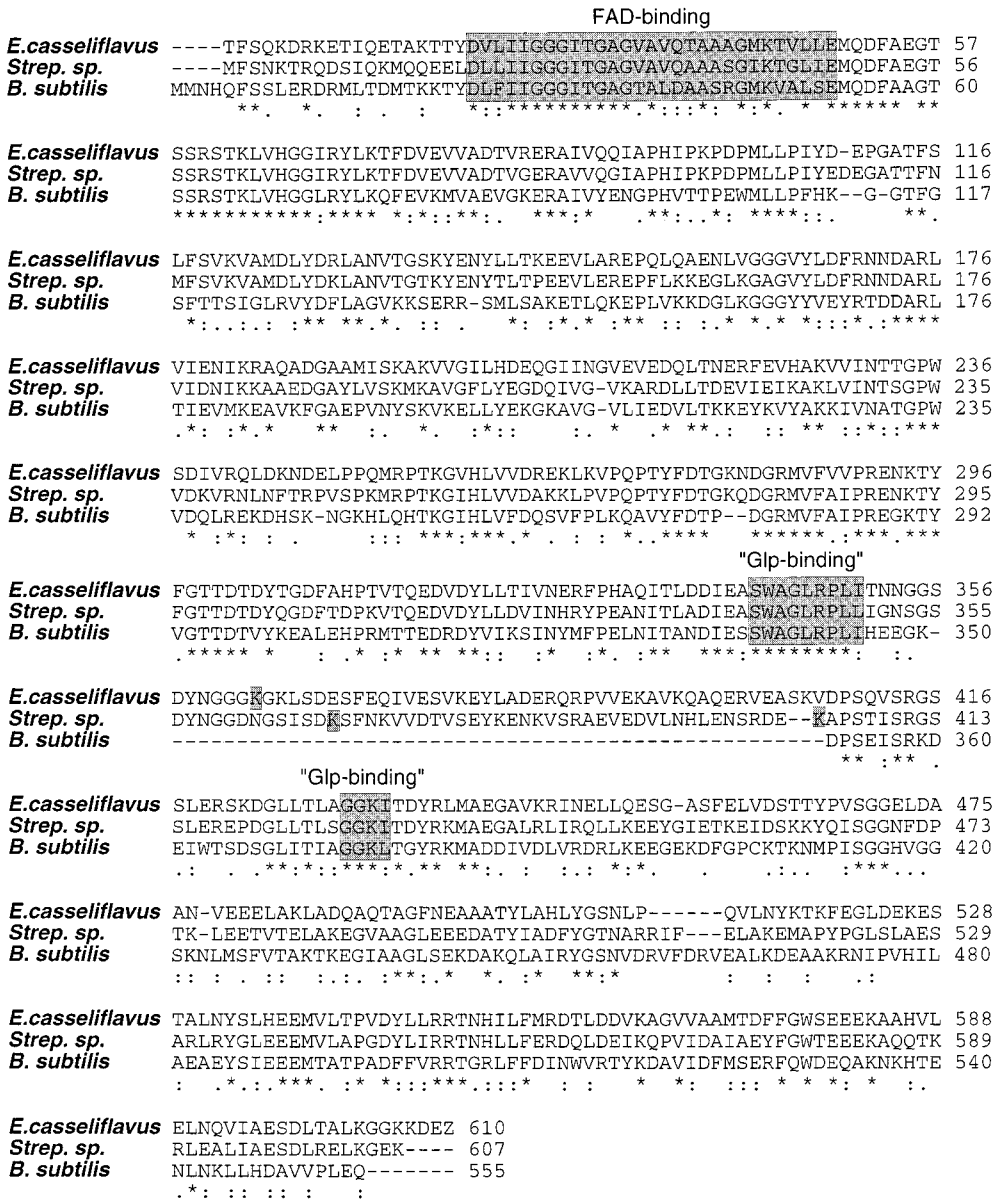

FIGURE 1: CLUSTAL alignment comparing GlpOs from *E. casseliflavus* and *Streptococcus* sp. with the *B. subtilis* GlpD. Asterisks indicate identical amino acids, while colons and periods represent similarities based on the evolutionary distances between amino acids. Boxes represent FAD-binding and putative "Glp-binding" segments, and the major trypsin cleavage sites identified for the GlpOs (Lys363 and Lys368/Lys404, respectively) are shaded.

GlpOs along with the *Bacillus subtilis* GlpD (*12*). The two GlpO sequences are 62% identical, and the insert region of GlpO-*S* corresponds to Ser355−Lys404; an alignment of the five known GlpO sequences shows that the insert segment is present in every case although shortened by two residues in GlpO-*S*. As expected, the FAD-binding segment at the N-terminus and the two putative Glp-binding sites are very strongly conserved. Like the *E. casseliflavus* enzyme, GlpO-*S* contains no Cys and only three Trp; these three Trp are absolutely conserved in the five GlpO sequences.

Limited Proteolysis of E. casseliflavus GlpO. A much earlier observation with the GlpO purified from *E. casseliflavus* had shown that treatment with trypsin led to the appearance of three major fragments of about 40, 26, and 28 kDa, and this was analyzed in detail with the recombinant enzyme as shown in Figure 2. By electroblotting the proteolysis products and analyzing their N-terminal sequences, it was established that the 40- and 28-kDa fragments

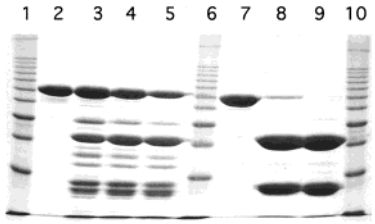

FIGURE 2: Limited proteolysis of *E. casseliflavus* (lanes 2−5) and *Streptococcus* sp. (lanes 7−9) GlpOs. *E. casseliflavus* GlpO is shown before (lane 2) and after 5, 10, and 15 min incubations (lanes 3−5) with trypsin (1:50 trypsin:GlpO, w/w) at 37 °C. *Streptococcus* sp. GlpO is shown before (lane 7) and after 5 and 15 min incubations (lanes 8 and 9) with trypsin (1:25 trypsin:GlpO, w/w) at 25 °C. Samples were analyzed on a 10% SDS−PAGE calibrated with the 10-kDa Protein Ladder standards (lanes 1, 6, and 10; the 20-kDa marker is visible at the dye front) as described in Experimental Procedures.

both retained the N-terminus of the intact protein (Table 1). The 26-kDa species shares the N-terminal sequence corre-

Table 1: Summary of N-Terminal and ESI-MS Data for Proteolysis of *E. casseliflavus* and *Streptococcus* sp. GlpOs

		molecular mass		peptide
	N-terminal sequence	ESI-MS (Da)	calculated (Da)	(cleavage site)
		A. *E. casseliflavus* GlpO		
intact protein	TFSQKDRKETI	67 082 ± 1	67 085	
40-kDa fragment	TFSQKD	40 005 ± 10	40 011	Thr2−Lys363 (K363)
28-kDa fragment	TFSQKDRKET	ND[a]		
26-kDa fragment	STkLVHGGIR[b]	ND		
		B. *Streptococcus* sp. GlpO		
intact protein	MFSNKTRQDSIQKMQQ	67 594 ± 8[c]	67 573	
40-kDa fragment	MFSNKT	40 511 ± 4	40 505	Met1−Lys368 (K368)
23-kDa fragment	(DEK)APSTIS	22 897 ± 2	22 895	Ala405−Lys607 (K404)
			(23 267)	(Asp402−Lys607) (R401)
25-kDa fragment	AEVEDVLNHLENSRDEK	ND	24 874	Ala388−Lys607 (R387)

[a] ND, not determined. [b] The yield of Lys in cycle 3 was lower than Ala, due to the presence of other peptide(s). [c] The increased mass (21 Da) is attributed to a Na^+ adduct (see text).

sponding to Ser61−Arg70 of the intact protein, consistent with cleavage at Arg60. Earlier ESI-MS analysis of the intact enzyme gave m = 67 082 Da, in excellent agreement with the calculated m of 67 085 Da (*2*). Table 1 also gives the result of a combined HPLC/ESI-MS analysis for the 40-kDa fragment, which allows the identification of Lys363 as the internal cleavage site. ESI-MS data were not obtained for the 26- and 28-kDa fragments of *E. casseliflavus* GlpO.

Limited Proteolysis of GlpO-S. Of the trypsin cleavage sites identified in the *E. casseliflavus* enzyme, Arg60 is conserved in GlpO-*S*, but Lys363 is replaced by Asn (Figure 1); while the Lys363 cleavage site does fall only eight residues into the *E. casseliflavus* GlpO insert and may be indicative of a flexible surface-exposed region of the protein, the relative complexity of these proteolysis profiles led us to investigate the readily available GlpO-*S*. In sharp contrast to the *E. casseliflavus* enzyme, proteolysis profiles for GlpO-*S* under the conditions described above gave much more favorable results. At 25 °C and a ratio of trypsin to GlpO-*S* of 1:25 (w/w), there was no residual intact GlpO at 15 min of incubation (Figure 2); in addition, the two major fragments of 40 and 23 kDa accounted for >90% of the total enzyme under these conditions.

As with the *E. casseliflavus* enzyme, the 40-kDa fragment of GlpO-*S* gave the same N-terminus (MFSNKT) as the intact protein (Table 1), while the 23-kDa band gave a mixture of two sequences in this analysis that differ only by a three-residue N-terminal extension of the latter; this corresponds to the segment (Asp402−Lys404)Ala405−Ser407 in GlpO-*S* and represents cleavages at both Arg401 and Lys404. Lys404 is the last residue within the GlpO-*S* insert segment. In view of the relatively straightforward proteolysis profile for GlpO-*S*, the ESI-MS analysis was carried out directly on a quenched reaction mixture that had been desalted on a CM-30 microconcentrator. SDS−PAGE analysis before and after ultrafiltration indicated no change in the profile for fragments ≥20 kDa, and an independent analysis using 16.5% gels and the Tris-Tricine buffer system failed to identify the anticipated 4.2-kDa peptide that would correspond to the excised GlpO-*S* fragment (see Discussion). As determined by ESI-MS, there are two major species present after proteolysis, and these correspond to m values of 40 511 ± 4 and 22 897 ± 2 Da, which in turn clearly represent the 40- and 23-kDa fragments seen on SDS−PAGE. The ESI-MS values are in excellent agreement with the calculated masses (from MS-DIGEST) of 40 505 and 22 895 Da for the fragments Met1−Lys368 and Ala405−Lys607, respectively. The absence of a 23 267-Da peptide (Asp402−Lys607) in the ESI-MS profile indicates that cleavage at Lys404 is essentially complete in this sample. Lys368 falls 14 residues into the GlpO-*S* insert; it should be noted that the first six residues (Ser355−Gly360 in GlpO-*S*) of the insert are absolutely conserved in the five known GlpOs, so the Lys363 cleavage site in *E. casseliflavus* GlpO follows this conserved segment by only two residues. In both GlpO and GlpO-*S*, the cleavage site is the first basic residue following this sequence.

We investigated the possible existence of additional conformational states involving the GlpO-*S* insert region by carrying out proteolysis reactions at relatively low concentrations of urea. GlpO-*S* was preincubated for 15 min at 25 °C with the appropriate urea concentration before trypsin was added, and the reaction was allowed to proceed for 15 min at 25 °C before quenching. At urea concentrations of 3 and 4 M, there was a progressive increase in a new peptide product of slightly higher apparent m (about 25 kDa) than the original 23-kDa band. There was no other significant change in the profile over 15 min, indicating that the protein maintains an essentially native conformation for at least 30 min in 4 M urea at 25 °C. When the 25-kDa polypeptide was electroblotted and sequenced (Table 1), it was determined that the presence of urea induces cleavage at Arg387. The calculated m for the expected Ala388−Lys607 fragment is 24 874, which is in excellent agreement with the SDS−PAGE analysis.

Spectroscopic and Redox Properties of Intact and Nicked GlpO-S. Visible absorption spectra of intact versus nicked GlpO-*S* are essentially identical at pH 7.0, and there is no hint of flavin loss during ultrafiltration. The observed retention of both 40- and 23-kDa fragments during ultrafiltration also suggests that these proteolysis products remain associated together with FAD. We have previously reported (*2*) that the bound FAD of *E. casseliflavus* GlpO is only 3% as fluorescent as free FAD; similar measurements indicate that intact GlpO-*S* is about 14% as fluorescent as the free coenzyme (λ_{EX} = 450 nm and λ_{EM} = 520 nm). Nicked GlpO-*S* exhibits a somewhat enhanced fluorescence (~21% that of free FAD); this does not reflect any significant contribution from free flavin, based on the essentially identical excitation spectra of intact and nicked enzymes.

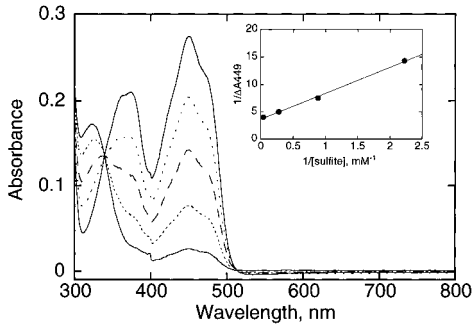

FIGURE 3: Sulfite titration of nicked GlpO-*S*. Nicked enzyme (24.5 μM, in 50 mM phosphate, pH 7.0, plus 0.5 mM EDTA) was titrated with sodium sulfite solutions of 0.1 and 1.0 M. Spectra shown in order of decreasing absorbance at 449 nm correspond to the addition of 0 (—), 0.45 (- -), 1.13 (— —), 3.6 (---), and 23 mM (—) total sulfite ($HSO_3^- + SO_3^{-2}$). Inset: Double-reciprocal plot of absorbance change at 449 nm versus added sulfite concentration.

GlpO from *E. casseliflavus* preferentially stabilizes the N(3)-anionic form of bound FAD; the pK_a is lowered to 8.5 (*5*). We examined the visible spectra of intact and nicked GlpO-*S* at pH values of 7.0, 8.5, and 10.0. In both cases, there is a significant increase in absorbance, along with a 20-nm blue shift for the near-UV absorbance maximum as the pH is increased to 8.5; these changes are quantitatively very similar to those originally seen with *E. casseliflavus* GlpO. The FAD N(3)-H pK_a value, however, seems to be decreased even further for GlpO-*S*, as there is very little absorbance change between pH 8.5 and pH 10.0. There is no significant change in this active-site pK_a with the nicked enzyme. GlpO-*S* has three Trp residues located at positions 235, 342, and 579. Trp342 falls within the strongly conserved segment, 13 residues ahead of the insert region, which has been implicated in Glp binding by the aerobic *Esc. coli* GlpD (*1*) on the basis of the TIM-DHAP structure. Trp579 is located toward the C-terminus shared by both the intact enzyme and the 23-kDa fragment. Both intact and nicked forms exhibit the same Trp fluorescence emission at 328 nm on excitation at 295 nm; proteolysis does not increase the solvent exposure of any of the three Trp residues.

The *E. casseliflavus* GlpO forms a stable flavin N(5)-sulfite adduct (K_d = 0.81 mM) at pH 7.0, 25 °C (*2*), and titrations of intact and nicked GlpO-*S* gave similar K_d values of 1.5 and 1.3 mM, respectively (Figure 3). Anaerobic titration of the enterococcal enzyme with dithionite at pH 7.0 leads to a mixture of relatively small amounts of both anionic and neutral flavin semiquinone intermediates; full reduction was reported to require 1.5−1.6 equiv of dithionite/FAD (*2*). The intact GlpO-*S* is reduced directly on titration with 1.1 equiv of dithionite, and there is essentially no evidence for stable semiquinone intermediates. The same behavior was observed with the nicked enzyme at pH 7.0. When intact GlpO-*S* was mixed anaerobically with 30 mM L-Glp, the enzyme was reduced completely within 25 s at pH 7.0, 25 °C, as monitored with a diode-array spectrophotometer (Figure 4). Over the next several minutes, however, the E-$FADH_2$ form of GlpO-*S* was converted to the red anionic semiquinone form in high yield. When the anaerobic cuvette was opened to air, there was some initial conversion back to E-$FADH_2$, but this was reversed completely within a few minutes. This is in marked contrast to the behavior of nicked GlpO-*S*, which only gives moderate yields of anionic

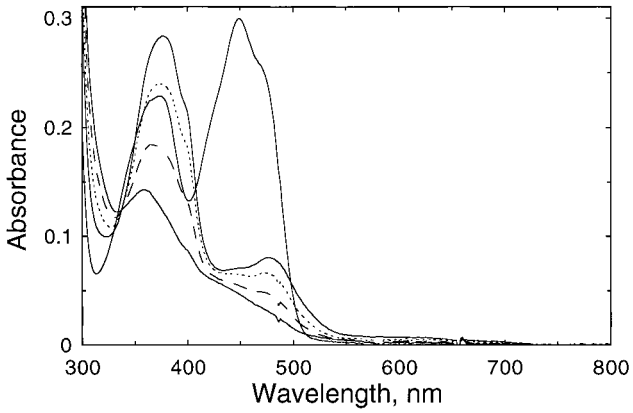

FIGURE 4: Anaerobic substrate reduction of intact GlpO-*S*. Intact enzyme (26.1 μM in the pH 7.0 phosphate/EDTA buffer) was mixed anaerobically with 30 mM L-Glp; spectra shown correspond to oxidized enzyme (—) and, in order of increasing absorbance at 375 nm, reduced enzyme at 25 (—), 85 (— —), and 210 s (- -) and 8 h (—) after mixing. The oxygen-scrubbing system consisting of protocatechuate dioxygenase and protocatechuic acid was added anaerobically prior to mixing.

semiquinone after exposure of the substrate-reduced enzyme to air. Since semiquinone does not accumulate with either intact or nicked GlpO-*S* during dithionite titration, it appears that the DHAP product may be an essential factor in the radical stabilizations described above.

Limited attempts to resolve the 40- and 23-kDa fragments of GlpO-*S* were made using anion exchange chromatography on a Mono Q column and gel filtration with Sephadex G-100 in the presence of 3.5 M urea, but in neither case was separation achieved. These results are consistent with the observation that ultrafiltration did not change the SDS−PAGE profile for fragments ≥20 kDa and again support a reasonably tight association together with FAD for the nicked enzyme fragments at concentrations of >1 μM. However, when measured in the standard spectrophotometric assay at nanomolar concentrations, the activity of nicked GlpO-*S* was only 3−4% that of intact enzyme. Considering that Triton X-100 is present to solubilize the *o*-dianisidine oxidation product, we investigated the possibility that the detergent could dissociate nicked GlpO-*S* fragments at 1−10 μM enzyme concentration, using both tryptophan and flavin fluorescence. While no direct evidence at these relatively high enzyme concentrations for a Triton-induced dissociation was obtained, we were unable to perform these spectroscopic analyses at nanomolar enzyme concentration as present in the standard assay. To avoid the potential for nicked GlpO-*S* dissociation at these low concentrations and to allow much better correlation between kinetic analyses and static spectral measurements at enzyme concentrations ≥10 μM, we employed the enzyme-monitored turnover method (*13*) with both intact and nicked GlpO-*S*.

Enzyme-Monitored Turnover Analyses. With the enzyme from *E. casseliflavus*, enzyme-monitored turnover analyses revealed that at steady state GlpO remains largely oxidized, even at 50 mM L-Glp; subsequent studies confirmed that reduction was essentially rate-limiting in turnover (*2*). The intact GlpO-*S* exhibits quite different behavior as revealed in diode-array and single-wavelength analyses of turnover with 10 μM enzyme and 0.77 mM O_2 over the L-Glp concentration range of 5−50 mM (pH 7.0, 5 °C). Even at

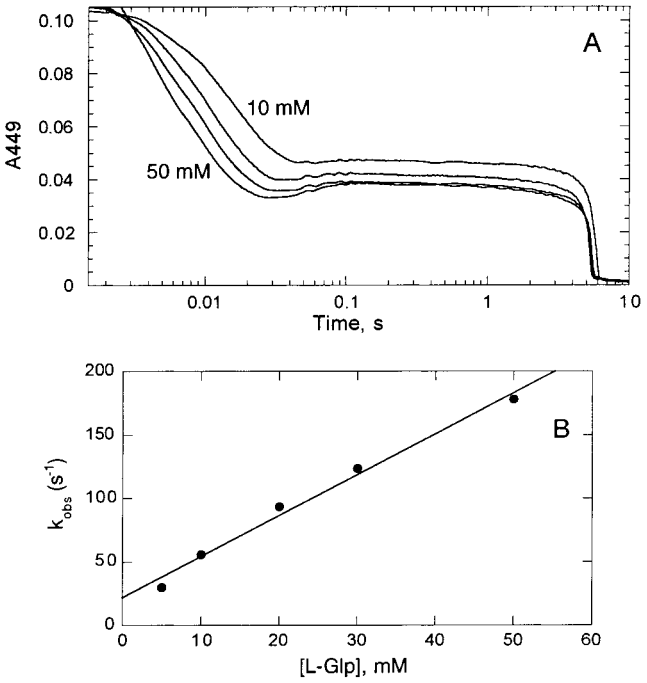

FIGURE 5: Enzyme-monitored turnover of intact GlpO-*S*. (A) Intact enzyme (10.3 μM after mixing, in air-equilibrated 0.1 M phosphate, pH 7.0, plus 0.5 mM EDTA) was mixed at 5 °C with different concentrations of L-Glp (5, 10, 20, 30, and 50 mM) that had been equilibrated with 100% O_2 in the same buffer. Final Glp concentrations are given for four selected traces, and the reactions were followed at 449 nm. (B) Direct plot of k_{obs} for the approach to steady state versus [Glp].

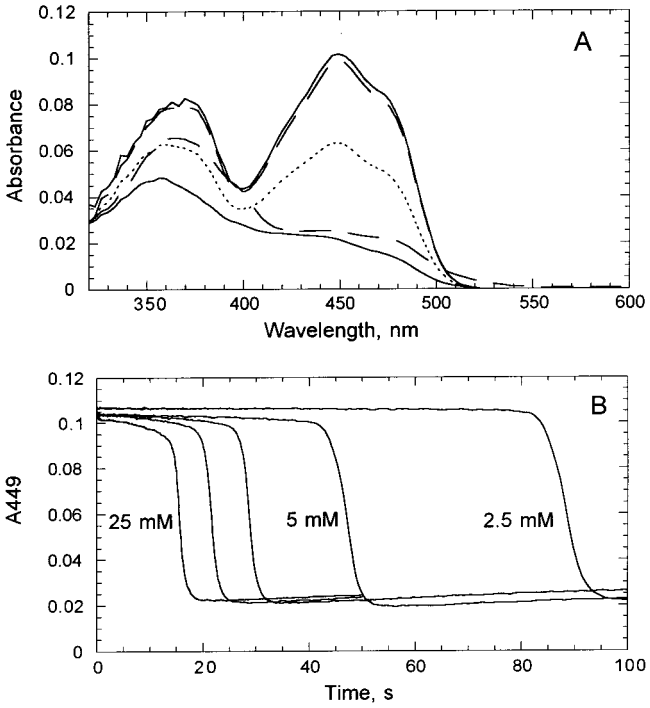

FIGURE 6: Enzyme-monitored turnover of nicked GlpO-*S*. (A) Nicked enzyme (9.5 μM) was mixed in the presence of 0.77 mM O_2 with 2.5 mM L-Glp as described in Figure 5, and the reaction was monitored by diode-array detection. Spectra correspond to the reaction mixture at 89 ms (—), 15 (— —) and 92 s (---), and the fully reduced enzyme 107 s after mixing (—). Also shown is the time-dependent formation of anionic semiquinone (500 s; — —) from reduced enzyme. (B) A_{449} traces for these reactions (at 2.5, 5, 10, 15, and 25 mM L-Glp) are given along with the corresponding L-Glp concentrations.

10 mM Glp, the enzyme is about 55% reduced at steady state (Figure 5), suggesting that K_m(Glp) is significantly lower than the value of 24 mM determined with the *E. casseliflavus* enzyme. The enzyme becomes fully reduced 6 s after mixing, once the limiting O_2 substrate has been depleted; at this time, it should be emphasized that none of the red anionic semiquinone seen in the anaerobic tip experiments described earlier is observed. By analyzing the data from these reactions as monitored at 449 nm, plots of $[O_2]/v$ versus $[O_2]$ (*14*) resulted in a pattern of lines that intersect on the *y* axis, consistent with a ping-pong mechanism. The secondary plot of [L-Glp]/V_{app} versus [L-Glp] gives K_m(Glp) and V_{max}; at pH 7.0, 5 °C, K_m(Glp) = 1.9 mM, $K_m(O_2)$ = 52 μM, and k_{cat} = 17.9 s^{-1}. While $K_m(O_2)$ and k_{cat} both differ from the respective parameters for *E. casseliflavus* GlpO by ≤2-fold, K_m(Glp) for GlpO-*S* is almost 13-fold lower than with the *E. casseliflavus* enzyme, consistent with the respective spectral properties in steady-state turnover. As described by Gutfreund (*15*), the approach to steady state for a simple flavoprotein should correspond to an apparent rate constant (k_{app}) equal to the sum of the first-order rate constants for the reduction and the reoxidation of the flavin. As shown in Figure 5, the monophasic approach to steady state expected with intact GlpO-*S* is complicated by the presence of a second kinetic phase, especially at high L-Glp concentrations. In our analyses, we have focused on the major ΔA_{449} component corresponding to GlpO-*S* reduction. When the corresponding k_{obs} values are analyzed over the Glp concentration range of 5−50 mM, a linear relationship is indicated with $k_{app} = 3.2 \times 10^3$ M^{-1} s^{-1} and a *y*-axis intercept of 21.7 s^{-1} (Figure 5). The first-order rate constant is very close to k_{cat} (17.9 s^{-1}) and suggests that DHAP release from E-$FADH_2$ may be limiting for both turnover and for reoxidation. By taking k_{red} = 32 s^{-1} at 10 mM L-Glp and k_{ox} = 21.7 s^{-1} as the limiting step in reoxidation, one can calculate that 60% of the total GlpO-*S* should be reduced at steady state. This agrees well with the 55% reduction observed experimentally, and these results will be discussed further in the context of the reductive half-reaction analysis.

The nicked enzyme displays several very different features in turnover, as analyzed by diode-array detection under conditions very similar to those used for intact GlpO-*S*. At 2.5 mM L-Glp, the enzyme at steady state is essentially fully oxidized (Figure 6), a direct indication that K_m(Glp) is increased significantly in the nicked enzyme and that the ratio k_{red}/k_{ox} is much lower than with intact enzyme. Furthermore, at this substrate concentration, the nicked enzyme requires almost 100 s to deplete the O_2 substrate; as the reaction mixture is monitored over the time frame of 100−500 s, the red anionic semiquinone described earlier clearly begins to develop in the absence of O_2. A very similar pattern is seen at 25 mM L-Glp; the enzyme remains largely oxidized in steady state, and even more anionic semiquinone is seen to accumulate after O_2 depletion. These reactions were then monitored with 0.77 mM O_2 over the L-Glp concentration range of 2.5−25 mM at 449 nm (Figure 6), and the kinetic data again are consistent with a ping-pong mechanism. Values for $K_m(O_2)$ and k_{cat} of 69 μM and 14.1 s^{-1} compare favorably with those for intact enzyme, but K_m(Glp) for the nicked enzyme is 36.2 mM, or 19-fold higher than

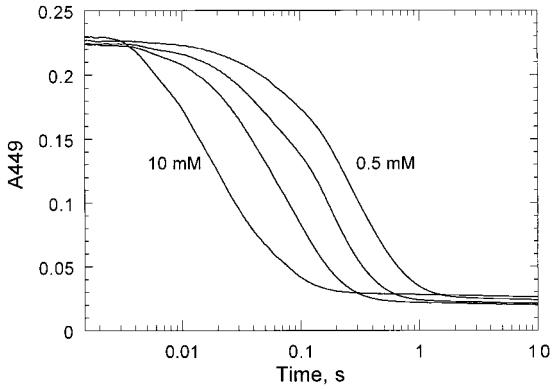

FIGURE 7: Reductive half-reaction of intact GlpO-*S*. Intact enzyme (27.6 μM final concentration) was reacted with substrate in the stopped-flow spectrophotometer under anaerobic conditions at pH 7.0, 5 °C. Final L-Glp concentrations for the traces shown were 0.5, 1, 2, and 10 mM.

with intact GlpO-*S*. Still, at infinite [L-Glp], k_{cat} for nicked enzyme is at least 80% that of intact GlpO-*S*. As expected, the respective k_{cat}/K_m(Glp) parameters reflect the large increase in K_m(nicked); to the extent that these represent lower limits for the respective second-order rate constants for association of Glp and E-FAD, the values are 9.4×10^3 and 390 M^{-1} s^{-1} for intact and nicked enzymes, respectively.

Reductive Half-Reaction Studies. Analyses of the reductive half-reaction with intact GlpO-*S* reveal no significant biphasic behavior at [Glp] $\leq K_m$. When these anaerobic reactions were analyzed at 449 nm over the L-Glp concentration range of 0.5−10 mM (Figure 7), however, k_{red} was taken either directly from the single-exponential fits at concentrations ≤2 mM or from the faster phase observed at 5 and 10 mM Glp. When these k_{red} values were analyzed versus L-Glp concentration, it was found that a direct plot of k_{red} accommodated the data very satisfactorily (Figure 8), giving a second-order rate constant of 4.9×10^3 M^{-1} s^{-1} for the essentially irreversible process at pH 7.0, 5 °C. It should be noted that this value compares reasonably well with $k_{app} = 3.2 \times 10^3$ M^{-1} s^{-1} from the approach to steady state. At 449 nm, the reduction traces at 10 mM L-Glp yield an average value for $k_{slow} = 11.7$ s^{-1} from two independent experiments; the magnitude of this rate constant approaches $k_{cat} = 17.9$ s^{-1} and suggests that it represents the rate-limiting step in the catalytic cycle. We presently conclude that this corresponds to the dissociation of DHAP from E-$FADH_2$. The kinetic mechanism for Glp reduction of intact GlpO-S thus differs significantly from that determined for the *E. casseliflavus* enzyme (*2*), in that there is no direct indication for a classical Michaelis complex between E-FAD and Glp, and DHAP release is essentially rate-limiting in turnover.

We then proceeded to analyze the reductive half-reaction of nicked GlpO-*S*, using both diode-array and 449-nm detection under anaerobic conditions. Diode-array analyses indicated that at a reaction time of 20 s with 10 mM L-Glp about 14% of the flavin had not been reduced, in comparison with diode-array spectra from enzyme-monitored turnover measurements with another nicked enzyme preparation, and similar results were obtained with 50 mM L-Glp. Otherwise the spectral course of reduction was very similar to that seen with intact enzyme, although the rate of reduction was much slower. When these reactions were analyzed at 449 nm over the L-Glp concentration range of 10−50 mM, distinctly

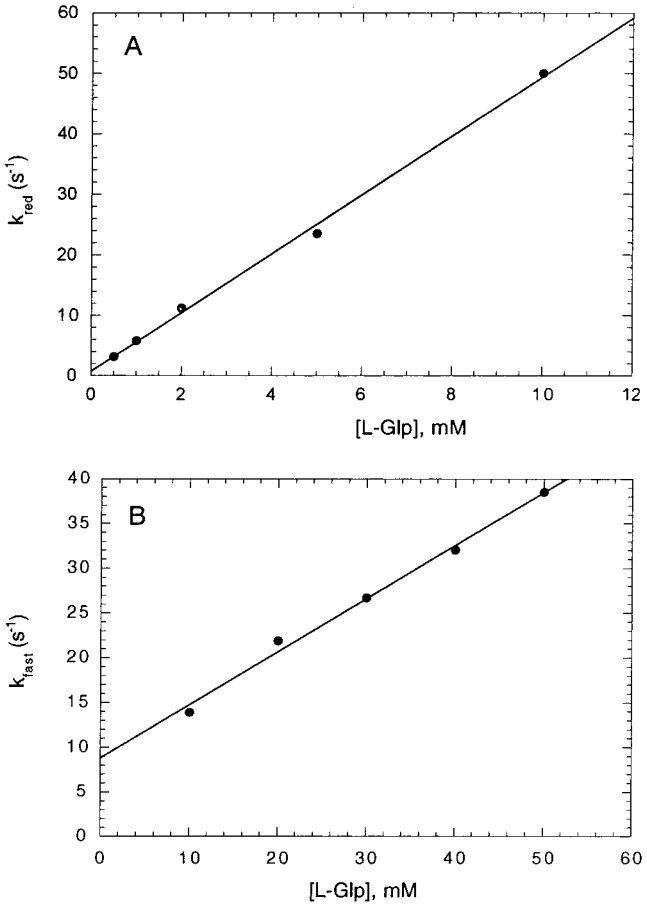

FIGURE 8: Kinetic analyses of the Glp reduction rates for intact and nicked GlpO-*S*. (A) Direct plot of k_{red} versus [L-Glp] is given for intact enzyme; values for k_{red} were determined from two nearly identical experiments as described in Figure 7 and in the text. (B) Direct plot of k_{fast} versus [L-Glp] is given for nicked enzyme; values for k_{fast} were determined in an experiment similar to that described in Figure 7 but using 21.6 μM nicked GlpO-*S* and L-Glp concentrations of 10, 20, 30, 40, and 50 mM. Other details are given in the text.

biphasic traces were observed in every case. The faster phase accounted for 37−47% of the total ΔA_{449} at 10−50 mM Glp; over this same range, the rate constant for the slow phase was essentially unchanged (1.8 to 2.6 s^{-1} at 5 °C); k_{slow} is also significantly less than the turnover number of 14.1 s^{-1}. In contrast, when the values for k_{fast} are analyzed versus [L-Glp] in a direct plot, a second-order rate constant of 590 M^{-1} s^{-1} with a finite *y*-axis intercept of 8.8 s^{-1} is obtained (Figure 8). This analysis (*16*) is indicative of a significant reversible component to the reduction of nicked GlpO-*S* not seen with the intact enzyme; furthermore, the corresponding second-order rate constant is decreased by more than 8-fold relative to that for intact GlpO-*S*. The slower rate of reduction observed with the nicked enzyme is consistent with the altered steady-state behavior in enzyme-monitored turnover analyses as described earlier.

DISCUSSION

Limited proteolysis of *Streptococcus* sp. GlpO leads to a dramatic change in the interaction between the resulting nicked enzyme and Glp. The kinetic parameters for steady-state and reductive half-reaction analyses of the intact and nicked GlpO-*S* forms are summarized in Tables 2 and 3. To

Table 2: Kinetic Constants for Intact and Nicked Forms of *Streptococcus* sp. GlpO

	intact GlpO-*S* from		nicked GlpO-*S* from	
term	steady state[a]	stopped-flow[b]	steady state[c]	stopped-flow[b]
K_m(Glp) (mM)	1.9	2.4	36.2	35.3
$K_m(O_2)$ (μM)	52	ND[d]	69	ND
k_{cat} (s^{-1})	17.9	11.7	14.1	(11.7)
$k_{cat}/K_m(O_2)$ ($M^{-1}\,s^{-1}$)	3.4×10^5		2.0×10^5	

[a] Calculated from the data in Figure 5. [b] Calculated from the appropriate values in Table 3, as described in the text and in refs *16* and *17*. [c] Calculated from the data in Figure 6. [d] ND, not determined.

begin with, there is a significant mechanistic difference in the reductive half-reactions of intact *E. casseliflavus* GlpO versus GlpO-*S*. The first indication that the interaction of Glp with intact GlpO-*S* is markedly different comes from the observation that K_m(Glp) is decreased from 24 mM with the *E. casseliflavus* enzyme to 1.9 mM with GlpO-*S*. Furthermore, analysis of the reductive half-reaction reveals that GlpO-*S* does not form a detectable Michaelis complex with Glp, reacting instead in a second-order fashion to yield the reduced enzyme·DHAP complex directly. This not only distinguishes GlpO-*S* from the *E. casseliflavus* enzyme but also differs from the kinetic pathway of the classical ping-pong mechanism (*16*). Similar behavior was seen on NADH reduction of the flavoprotein melilotate hydroxylase (*17*), where the reaction also corresponds to an irreversible second-order process. Our results with intact GlpO-*S* lead to the following kinetic mechanism:

$$\text{E-FAD} + \text{Glp} \underset{k_2}{\overset{k_1}{\rightleftharpoons}} \text{E-FADH}_2\cdot\text{DHAP} \underset{k_4}{\overset{k_3}{\rightleftharpoons}} \text{E-FADH}_2 + \text{DHAP}$$

$$\text{E-FADH}_2 + \text{O}_2 \xrightarrow{k_5} \text{E-FAD} + \text{H}_2\text{O}_2$$

By comparison with the melilotate hydroxylase mechanism, $\emptyset_{Glp} = (k_2 + k_3)/k_1k_3$, but since the direct plot of k_{red} versus [L-Glp] reveals that $k_2 = 0$ this expression simplifies to $1/k_1$. As described in Results, the slower phase observed with intact GlpO-*S* during reduction at high L-Glp concentrations has been attributed to the release of DHAP from reduced enzyme (k_3). In view of the second-order reaction between Glp and E-FAD, we presently conclude that this product dissociation step is essentially rate-limiting in turnover; thus $k_3 \sim k_{cat}$ (and $\emptyset_0 \sim 1/k_3$). The corresponding values for $\emptyset_0$ and $\emptyset_{Glp}$ can be calculated from the rate constants presented in Table 3; when taken together, they yield a calculated value for K_m(Glp) of 2.4 mM (Table 2), which agrees satisfactorily with the experimental value (1.9 mM) determined from the data of Figure 5. Thus, there is generally quite good agreement between the steady-state parameters and the mechanism as supported by the reductive half-reaction analysis. Note that while we have not directly determined k_5, the rate constant for reoxidation of reduced GlpO-*S*, the $k_{cat}/K_m(O_2)$ value of 3.4×10^5 M^{-1} s^{-1} at pH 7.0, 5 °C, does provide a lower limit and compares favorably with that determined for *E. casseliflavus* GlpO (1.1×10^6 M^{-1} s^{-1}) under similar conditions (*2*). The very close agreement in these values between intact and nicked forms of GlpO-*S* furthermore indicates that the oxidative half-reaction is not significantly affected by limited proteolysis.

Analysis of the reductive half-reaction with nicked GlpO-*S* reveals a change in kinetic mechanism such that there is now a significant reversible component ($k_2 = 8.8$ s^{-1}) to the second-order reaction, and k_1 is decreased over 8-fold relative to the intact GlpO-*S*. Given the smaller individual k_{red} values measured versus L-Glp concentration in this case, we did not directly observe the DHAP release step that was seen with the intact enzyme at high substrate concentration ($k_3 = 11.7$ s^{-1}). For this reason, and given the very favorable comparison between k_{cat} values for intact and nicked GlpO-*S* forms, we have also assigned a value of $k_3 = 11.7$ s^{-1} for the nicked enzyme. Taking $\emptyset_{Glp} = (k_2 + k_3)/k_1k_3$, the stopped-flow value of 3.0×10^{-3} M·s is in very good agreement with the steady-state value of 2.6×10^{-3} M·s. Furthermore, when the stopped-flow value for $\emptyset_{Glp}$ is taken together with $\emptyset_0$ ($= 1/k_3$), the value calculated for K_m(Glp) (= 35.3 mM) is in excellent agreement with the steady-state value of 36.2 mM.

The value for k_{slow} measured in the reductive half-reaction with nicked enzyme is independent of Glp concentration, ranging from 1.8 to 2.6 s^{-1} over a 5-fold increase in substrate concentration. The corresponding amplitudes in the ΔA_{449} traces account for 53−63% of the total change on reduction. $k_{slow} \ll k_{cat}$ (14.1 s^{-1}), and at the same time, these values are very similar to the rate constants of 3.6−5.4 s^{-1} as determined for k_{slow} in the reductive half-reaction of *E. casseliflavus* GlpO; the amplitudes represented by k_{slow} in that case were 13−35% of the total ΔA_{446} (*2*). No comparable behavior was observed in the steady-state analysis of nicked GlpO-*S*, and we presently interpret this result to indicate that the resting oxidized form of nicked, but not intact, GlpO-*S* exists in 2 states that are distinct in their abilities to bind L-Glp productively for reduction:

$$\text{E-FAD*} \underset{k_{11}}{\overset{k_{10}}{\rightleftharpoons}} \text{E-FAD} \underset{k_2}{\overset{k_1[\text{Glp}]}{\rightleftharpoons}} \text{E-FADH}_2\cdot\text{DHAP}$$

where reduction of E-FAD* is limited by $k_{10} = 1.8-2.6$ s^{-1}. The ratio of the amplitudes (ΔA_{449}) corresponding to k_{fast} and k_{slow} ($= k_{10}$) at saturating [L-Glp] should equal k_{10}/k_{11}; at 50 mM substrate concentration, this gives $k_{10}/k_{11} = 0.9$, which can be compared with the value of 6.7 for *E. casseliflavus* GlpO at 50 mM L-Glp.

As discussed by Creighton (*18*), limited proteolysis results such as those described for GlpO-*S* are generally indicative of either a flexible polypeptide segment linking independent structural domains or an exposed flexible polypeptide loop on the surface of the folded protein. Even in the latter case, the folded conformation of the nicked protein often remains stable. Long, flexible loop regions frequently adopt different conformations, such as the open and closed forms of TIM (*4*, *19*, *20*); still, the flexible loop of TIM (10−14 residues) is much shorter than the 50−52 residue insert found in GlpO. Focusing on the proteolysis results with GlpO-*S*, the intact enzyme is a dimer with subunit $m = 67.6$ kDa (not including the bound flavin). The results of proteolysis, gel filtration, and spectroscopic analyses indicate that the core dimers of both intact and nicked GlpO-*S* are relatively stable in the presence of 4 M urea. In the absence of urea, trypsin cleaves primarily at Lys368 and Lys404, generating two major

Table 3: Rate Constants for Reductive Half-Reactions of Intact and Nicked GlpO-*S* and Correlation of Steady-State and Stopped-Flow Results[a]

		intact GlpO-*S* from		nicked GlpO-*S* from	
term	kinetic equivalent[b]	steady-state[c]	stopped-flow	steady-state[d]	stopped-flow
k_1 (M^{-1} s^{-1})			4.9×10^3		590
k_2 (s^{-1})			0		8.8
k_3 (s^{-1})			11.7		(11.7)
k_4			ND[e]		ND
$Ø_0$ (s)	$1/k_3$	5.6×10^{-2}	8.5×10^{-2}	7.1×10^{-2}	(8.5×10^{-2})
$Ø_{Glp}$ (M·s)	$(k_2 + k_3)/k_1k_3$	1.1×10^{-4}	2.0×10^{-4}	2.6×10^{-3}	3.0×10^{-3}

[a] See the text for identification of each step. Except where noted, each rate constant was measured directly in the stopped-flow spectrophotometer at 5 °C. [b] Assuming the mechanism described in the text. [c] Calculated from the data in Figure 5. [d] Calculated from the data in Figure 6. [e] ND, not determined.

fragments: Met1−Lys368, $m = 40.5$ kDa; and Ala405−Lys607, $m = 22.9$ kDa. Attempts to identify the expected 4.2-kDa product corresponding to Ser369−Lys404 were not successful, suggesting that this fragment has dissociated from the core protein and been subjected to further proteolysis (there are five internal Lys + Arg). At concentrations ≥1 μM, our collected spectroscopic and other static analyses of the nicked enzyme indicate that the two major fragments remain tightly associated together with FAD; there is no significant change in active-site properties as indicated both in titrations with dithionite and sulfite and in preferential binding of the N(3)-anionic form of FAD. There is no change in the environments of any of the three Trp per GlpO-*S* monomer, including that of Trp579, which is located near the C-terminus of the 22.9-kDa fragment. Given the evidence for binding of FAD by an N-terminal segment of GlpO-*S*, it seems very likely that the ability of the nicked enzyme to retain the tightly bound coenzyme even in the presence of 4 M urea is a significant factor in stabilizing the folded core conformation against further proteolysis. The only effect of urea at this concentration is to direct cleavage at Arg387 instead of Lys404 in a portion of the GlpO-*S* molecules; this yields a larger C-terminal fragment of about 25 kDa and most likely reflects a rather localized structural perturbation caused by the denaturant that has no effect on cleavage at Lys368. At nanomolar enzyme concentrations in the presence of Triton X-100 at 25 °C, nicked GlpO-*S* only exhibits 3−4% activity as compared to intact enzyme; this observation does suggest that the GlpO-*S* fragments and/or FAD dissociate at nanomolar concentrations under these conditions.

Whether proteolytic excision of the GlpO-*S* insert reflects the presence of flexible surface loop(s) within this segment or simply indicates a role in linking independent structural domains, two recent studies employing limited proteolysis as a structural probe of the flavoenzymes DHOD and DAAO provide clear evidence for active-site loops that play important roles in substrate binding and/or dehydrogenation. With the membrane-associated *Esc. coli* DHOD, trypsin cleaves specifically at Arg182 (*21*); although the resulting 22- and 18-kDa fragments of the multimeric enzyme remained associated together with FMN, the nicked enzyme only retained 0.5% activity with quinone acceptor substrates. Anaerobic stopped-flow analyses of the reduction of intact and nicked DHODs demonstrated that although dihydroorotate binds the nicked enzyme, only very slow and incomplete flavin reduction was observed. The Arg182 cleavage site comes at the end of a nine-residue segment in DHOD that corresponds very closely to the *Lactococcus lactis* DHODA active-site loop structure (*22*). Binding of the product orotate has been demonstrated to cause a significant reduction in the mobility of this loop (*23*), which shields the substrate-binding site from solvent. Substrate binding therefore seems to require a significant opening of the surface loop, as apparently occurs even with nicked DHOD. The catalytic defect is associated with an impaired capability for proton abstraction and/or hydride transfer from the bound dihydroorotate (*21*). Similar studies with DAAO demonstrated that cleavage with trypsin at Arg221 led to 25- and 13.4-kDa products (*24*, *25*). As with GlpO-*S* and DHOD, these fragments remained associated together with the flavin. The competitive inhibitor benzoate completely protected against this cleavage, but even in the absence of benzoate there was always a residual core of 30% of the enzyme resistant to proteolysis. These results were correlated, along with extensive steady-state kinetic analyses with three substrates, with the crystal structure of the DAAO−benzoate complex (*26*). Arg221 falls within the active-site loop consisting of residues 216−228; benzoate binding orders the loop such that its closed conformation, which is not accessible to trypsin, is stabilized. In a similar manner, this loop has been implicated in a conformational change necessary for both substrate binding and product dissociation. The loss of activity observed specifically with D-Ser on proteolysis was taken to represent the absence of a coordinated loop movement required during closure of the active site on D-Ser binding, leading to a large increase in k_{off} for this substrate (*25*).

As discussed by Mattevi et al. (*27*), catalysis very often takes place in cavities buried below the protein surface, and conformational changes as expressed by active-site loops or lids as seen in DHOD and DAAO, as well as TIM and a host of other enzymes, must accompany substrate binding and/or product dissociation. As has been proposed for both DHOD (*23*, *28*) and DAAO (*26*, *27*), the GlpOs operate by a hydride transfer mechanism in which a proton is abstracted from the substrate C(2)-hydroxyl, leading to the elimination of $H:^-$ and the commensurate formation of E-$FADH_2$ and DHAP (*2*, *5*). The relative positioning of the substrate and the flavin is a critical factor for optimal catalysis, as is the maintenance of the solvent-protected cavity; Stoll et al. (*29*) have pointed out that effective hydride transfer can only occur within a hydrophobic environment. The closure of the active-site loops in DHOD and DAAO should also facilitate substrate dehydrogenation by shielding the active site from solvent. While the present study does not prove the existence of such a functional, flexible loop in the GlpO-*S* active site,

[2] C. M. Finnerty and P. A. Karplus, personal communication.

it is important to recall (a) that the GlpO insert falls between two segments of the polypeptide previously implicated in Glp binding to the *Esc. coli* GlpD (*1*); (b) that the nicked GlpO-*S* exhibits a marked change in the kinetic mechanism for enzyme reduction (i.e., hydride transfer to FAD), including a >8-fold decrease in k_1; and (c) that the nicked enzyme also exhibits a dramatic increase in that reduction component limited by k_{10}, the rate constant for the conformational conversion of E-FAD* → E-FAD. Each of these observations is consistent with an important catalytic role for this segment in GlpO-*S*, which can be compared with the flexible loops in DHOD and DAAO. It should also be emphasized that despite the importance of Glp in intermediary metabolism and in the shuttling of cytosolic reducing equivalents to the mitochondria (*30*), very little is known about Glp recognition and binding to enzymes involved in this aspect of energy metabolism. To advance our understanding of this and other aspects of GlpO structure and function, the intact GlpO-*S* has recently been crystallized, and a 90% complete data set has been collected to 2.8 Å resolution.[2]

ACKNOWLEDGMENT

We thank Dr. Hideo Misaki for providing the sequence of *Streptococcus* sp. GlpO and Dr. Kazuko Yorita for her invaluable help in facilitating this exchange. We thank Dr. Mike Thomas and Mr. Mike Samuel for providing the mass spectrometry analyses and Dr. Mark Lively for providing the protein sequence analyses.

REFERENCES

1. Austin, D., and Larson, T. J. (1991*) J. Bacteriol. 173*, 101−107.
2. Parsonage, D., Luba, J., Mallett, T. C., and Claiborne, A. (1998) *J. Biol. Chem. 273*, 23812−23822.
3. Dolin, M. I. (1961) in *The Bacteria* (Gunsalus, I. C., and Stanier, R. Y., Eds.) Vol. II, pp 425−460, Academic Press, New York.
4. Alber, T. C., Davenport, R. C., Jr., Giammona, D. A., Lolis, E., Petsko, G. A., and Ringe, D. (1987*) Cold Spring Harbor Symp. Quant. Biol. 52*, 603−613.
5. Claiborne, A. (1986) *J. Biol. Chem. 261*, 14398−14407.
6. *User Bulletin* (1993) No. 58, PE Biosystems, Foster City, CA.
7. *Life Science Research Products* (2000) Bio-Rad Laboratories, Hercules, CA.
8. Baker, P., and Clauser, K. (1999) MS-Digest, http://prospector.ucsf.edu/ucsfhtml3.2/msdigest.htm.
9. Luba, J., Charrier, V., and Claiborne, A. (1999) *Biochemistry 38*, 2725−2737.
10. Pajot, P. (1976) *Eur. J. Biochem. 63*, 263−269.
11. Mallett, T. C., and Claiborne, A. (1998) *Biochemistry 37*, 8790−8802.
12. Holmberg, C., Beijer, L., Rutberg, B., and Rutberg, L. (1990) *J. Gen. Microbiol. 136*, 2367−2375.
13. Gibson, Q. H., Swoboda, B. E. P., and Massey, V. (1964) *J. Biol. Chem. 239*, 3927−3934.
14. Cornish-Bowden, A. (1995) *Fundamentals of Enzyme Kinetics*, Portland Press, London.
15. Gutfreund, H. (1972) *Enzymes: Physical Principles*, John Wiley & Sons, New York.
16. Dalziel, K. (1957) *Acta Chem. Scand. 11*, 1706−1723.
17. Strickland, S., and Massey, V. (1973) *J. Biol. Chem. 248*, 2953−2962.
18. Creighton, T. E. (1993) *Proteins: Structures and Molecular Properties*, W. H. Freeman and Company, New York.
19. Lolis, E., Alber, T., Davenport, R. C., Rose, D., Hartman, F. C., and Petsko, G. A. (1990) *Biochemistry 29*, 6609−6618.
20. Wierenga, R. K., Noble, M. E. M., Postma, J. P. M., Groendijk, H., Kalk, K. H., Hol, W. G. J., and Opperdoes, F. R. (1991) *Proteins 10*, 33−49.
21. Björnberg, O., Grüner, A.-C., Roepstorff, P., and Jensen, K. F. (1999) *Biochemistry 38*, 2899−2908.
22. Rowland, P., Nielsen, F. S., Jensen, K. F., and Larsen, S. (1997) *Structure 5*, 239−252.
23. Rowland, P., Björnberg, O., Nielsen, F. S., Jensen, K. F., and Larsen, S. (1998*) Protein Sci. 7*, 1269−1279.
24. Tarelli, G. T., Vanoni, M. A., Negri, A., and Curti, B. (1990) *J. Biol. Chem. 265*, 21242−21246.
25. Vanoni, M. A., Cosma, A., Mazzeo, D., Mattevi, A., Todone, F., and Curti, B. (1997) *Biochemistry 36*, 5624−5632.
26. Mattevi, A., Vanoni, M. A., Todone, F., Rizzi, M., Teplyakov, A., Coda, A., Bolognesi, M., and Curti, B. (1996) *Proc. Natl. Acad. Sci. U.S.A. 93*, 7496−7501.
27. Mattevi, A., Vanoni, M. A., and Curti, B. (1997) *Curr. Opin. Struct. Biol. 7*, 804−810.
28. Hines, V., and Johnston, M. (1989) *Biochemistry 28*, 1227−1234.
29. Stoll, V. S., Kimber, M. S., and Pai, E. F. (1996) *Structure 4*, 437−447.
30. Garrett, R. H., and Grisham, C. M. (1999) *Biochemistry*, 2nd ed., Harcourt Brace & Company, Orlando, FL.

BI992499J